Published OnlineFirst August 24, 2017; DOI: 10.1158/1535-7163.MCT-17-0293

Small Molecule Therapeutics

Molecular Cancer Therapeutics

Animacroxam, a Novel Dual-Mode Compound Targeting Histone Deacetylases and Cytoskeletal Integrity of Testicular Germ Cell Cancer Cells

Gustav Steinemann[1], Alexandra Dittmer[1], Weronika Kuzyniak[1], Björn Hoffmann[1], Mark Schrader[2], Rainer Schobert[3], Bernhard Biersack[3], Bianca Nitzsche[1], and Michael Höpfner[1]

Abstract

Novel approaches for the medical treatment of advanced solid tumors, including testicular germ cell tumors (TGCT), are desperately needed. Especially, TGCT patients not responding to cisplatin-based therapy need therapeutic alternatives, as there is no effective medical treatment available for this particular subgroup. Here, we studied the suitability of the novel dual-mode compound animacroxam for TGCT treatment. Animacroxam consists of an HDAC-inhibitory hydroxamate moiety coupled to a 4,5-diarylimidazole with inherent cytoskeleton disrupting potency. Animacroxam revealed pronounced antiproliferative, cell-cycle arresting, and apoptosis-inducing effects in TGCT cell lines with different cisplatin sensitivities. The IC_{50} values of animacroxam ranged from 0.22 to 0.42 μmol/L and were not correlated to the cisplatin sensitivity of the tumor cells. No unspecific cytotoxicity of animacroxam was observed in either cisplatin-sensitive or resistant TGCT cells, even at doses as high as 10 μmol/L. Furthermore, animacroxam induced the formation of actin stress fibers in cancer cells, thereby confirming the cytoskeleton-disrupting and antimigratory properties of its imidazole moiety. When compared with the clinically established HDAC inhibitor vorinostat, the novel dual-mode compound animacroxam exhibited superior antitumoral efficacy *in vitro*. Animacroxam also reduced the tumor size of TGCT tumors *in vivo*, as evidenced by performing xenograft experiments on tumor bearing chorioallantoic membranes of fertilizes chicken eggs (CAM assay). The *in vivo* experiments also revealed a very good tolerability of the compound, and hence, animacroxam may be a promising candidate for innovative treatment of TGCT in general and the more so for platinum-insensitive or refractory TGCT. *Mol Cancer Ther; 16(11); 2364–74. ©2017 AACR.*

Introduction

In contrast to most other malignancies, testicular germ cell tumors (TGCT) occur early in life. They are the most common malignancy in males between 20 and 45 years of age (1). Up to 80% of patients with advanced or metastatic disease can be cured by cisplatin-based chemotherapy (2). However, 20% of the patients show or develop cisplatin resistance, associated with poor prognosis and long-term survival rates of only 30% (3, 4). Furthermore, recent studies indicate long-term consequences of platinum-based therapies, such as a higher risk to develop neurologic disorders, cardiovascular diseases, metabolic syndromes, kidney failure, pulmonary disorders (5, 6) or other secondary malignancies (7, 8). This emphasizes the urgency to develop new and platinum-free therapies for the treatment of testicular germ cell cancer.

The inhibition of histone deacetylases (HDAC) with small-molecule inhibitors has emerged as a new and promising approach for cancer treatment. HDACs play an important role in chromatin remodeling and are implicated in the epigenetic regulation of cellular metabolism, growth, and differentiation (9–12). Deacetylation of histones increases the binding of positively charged histones to the negatively charged DNA. This leads to a more condensed DNA structure that, in turn, prevents transcription.

Tumor cells of different origin, including breast-, prostate-, kidney, and also testicular cancer, show increased HDAC activity leading to the repression of tumor suppressor genes like CDKN1A (p21) and CDKN1B (p27) or DNA repair genes like TP53, which results in increased cell activity and loss of apoptosis (13–16). The connection between increased HDAC activity and HDAC-dependent dysregulation of genes in cancer is best described for acute promyelocytic leukemia (AML). HDAC inhibitors such as vorinostat (**s**uberoyl**a**nilide **h**ydroxamic **a**cid or SAHA) and romidepsin (Istodax) are already in clinical application for the treatment of AML (17, 18).

Another interesting morphologic target for novel cancer therapeutics is the cytoskeleton of tumor cells. It is composed of actin and intermediate filaments as well as microtubules that confer the structural integrity and adaptability of a cell. The filaments of the cytoskeleton facilitate intracellular transport as well as the fixation of cell organelles like mitochondria inside the cell, and they are involved in cell division. In addition, the cytoskeleton has been found to be involved in gene expression (19). In tumor cells, the cytoskeleton is often altered in its dynamic capacity to facilitate

[1]Charité – Universitätsmedizin Berlin, corporate member of Freie Universität Berlin, Humboldt-Universität zu Berlin, and Berlin Institute of Health, Institute of Physiology. [2]Clinic of Urology, Helios Clinic Berlin-Buch, Berlin, Germany. [3]Organic Chemistry Laboratory, University of Bayreuth, Bayreuth, Germany.

Note: B. Nitzsche and M. Höpfner are co-senior authors of this article.

Corresponding Author: Michael Höpfner, Institute of Physiology, Charité, Charitéplatz 1, Berlin 10117, Germany. Phone: 4930-4505-28515; Fax: 493-045-0528 918; E-mail: michael.hoepfner@charite.de

doi: 10.1158/1535-7163.MCT-17-0293

Published OnlineFirst August 24, 2017; DOI: 10.1158/1535-7163.MCT-17-0293

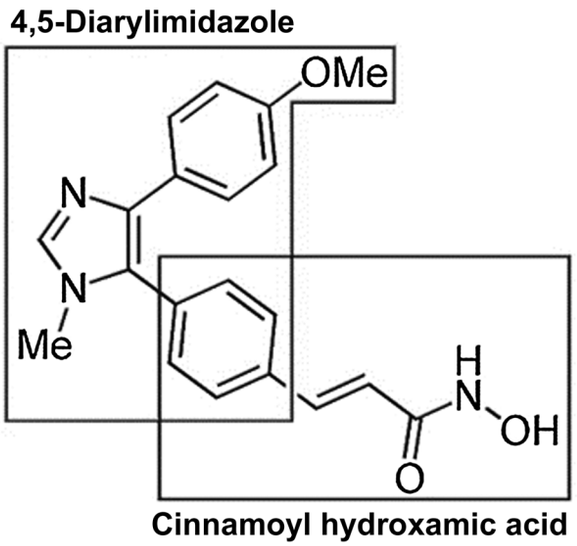

Figure 1.
Chemical structure of animacroxam. The dual mode inhibitor animacroxam consists of a cinnamoyl hydroxamic acid group linked to a 4,5-diarylimidazole moiety.

proliferation, migration, and metastasis formation. Targeting the dynamics of the cytoskeleton of tumor cells with specific modulators, such as tubulin polymerization inhibitors, is already in use for the therapy of TGCT. For instance, the tubulin-targeting Vinca alkaloid vinblastine is routinely given in combination with cisplatin and the antibiotic bleomycin (20).

The novel compound animacroxam (4-(1-methyl-4-anisyl-imidazol-5-yl)-*N*-hydroxycinnamide hydrochloride) (Fig. 1) was designed to combine the inhibition of HDAC activity and of the cytoskeletal dynamics of cancer cells. Animacroxam consists of a cinnamoyl hydroxamic acid, a prominent structural motif of second-generation HDAC inhibitors, linked to a 4,5-diarylimidazole, which is known to interfere with the integrity and dynamics of actin and microtubules of the cytoskeleton of transformed cells (21).

Hydroxamic acids are prominent (pan-)HDACi, and derivatives such as vorinostat, panobinostat, belinostat, and romidepsin have already been approved for the treatment of hematologic and lymphoid malignancies or are in advanced clinical development (22, 23). However, the disadvantage of HDACi containing only hydroxamic acids is that they are often leading to intrinsic drug resistance and could even promote tumor growth (21). To enhance the efficacy of the HDACi, we have combined the zinc-chelating hydroxamic acid fragment, which is common in many potent HDACi, with a 4,5-diarylimidazole moiety with proven anticancer activity in solid tumors. Moreover, the new imidazole-based derivatives were recently shown to be orally applicable and well tolerated in mice (24).

We now investigated the antitumoral effects of this new dual mode inhibitor in TGCT for the first time. Its capability to simultaneously act on different cell growth and survival mechanisms should diminish the probability of resistance as observed frequently for monotherapeutic agents like cisplatin or vorinostat (25, 26).

Materials and Methods

Compounds

Stock solutions of animacroxam (20 mmol/L), vorinostat (20 mmol/L), and cisplatin (3.3 mmol/L) were prepared in DMSO and stored at 4°C. Vorinostat was purchased from LC Laboratories and used without further purification. Animacroxam was prepared as a hydrochloride salt according to a literature procedure (27). Cisplatin was purchased from TEVA GmbH.

Cell culture and reagents

All TGCT cell lines were cultured in an incubator (5% CO_2, 37°C, humidified atmosphere). The nonseminoma (teratocarcinoma) cell line NCCIT was obtained from ATCC in 2013. 2102EP (nonseminoma, teratocarcinoma, and yolk-sack tumor) cells were kindly provided by Dr. F. Honecker (Tumor- und Brustzentrum ZeTuP, 9006 St. Gallen, Switzerland) in 2013. Cisplatin-resistant 2102EP-R cells were established by long-term culture of native 2102EP cells with sublethal concentrations of cisplatin as described earlier (28). New cells were thawed after passage 10 was reached. Cells were not tested for mycoplasma. NCCIT were cultured in DMEM UltraGlutamine medium (Lonza) supplemented with 10% FCS, 2 mmol/L L-glutamine, 50 U/mL penicillin, and 50 μg/mL streptomycin. 2102EP and 2102EP-R cells were cultured in DMEM/F12 (1:1) medium (Life Technologies Gibco) supplemented with 10% FCS, 2 mmol/L L-glutamine, 50 U/mL penicillin, and 50 μg/mL streptomycin.

Determination of cell proliferation

Crystal violet staining was performed to determine treatment-induced changes in TGCT cell numbers as described in a previous study (29). Briefly, 1.500 cells per well were seeded in 96-well plates for 24 hours at 37°C, 5% CO_2. Subsequently, cells were incubated with rising concentrations of animacroxam (0.1–3.2 μmol/L), vorinostat (0.1–10 μmol/L), or cisplatin (0.1–10 μmol/L) for up to 96 hours. Thereafter, the cells were fixed with 1% glutaraldehyde and stained with 0.1% crystal violet (Sigma-Aldrich). The unbound dye was removed by rinsing with water. Bound crystal violet was solubilized with 0.2% Triton X-100 (Sigma-Aldrich). Light extinction of crystal violet, which increases linearly with the cell number, was analyzed at 570 nm using an ELISA-Reader (Dynex Technologies). The experiments were performed in hexaplicate with $n = 5$.

Real-time monitoring of cell proliferation

2102EP and 2102EP-R (1.0×10^4 cells/well) and NCCIT cells (4.0×10^4 cells/well) were seeded in 8-well micro E-plates in 600 μL medium/well and maintained in an incubator for 24 hours to allow attachment. Thereafter, the cells were incubated with 0.25 to 2 μmol/L animacroxam for 72 hours. The iCELLigence system (ACEA Biosciences) was used to monitor proliferation of viable cells every 15 minutes for 96 hours in two PET 8-well plates, recording the cells' attachment through electronic sensors at the bottom of each well. Cell proliferation was recorded as arbitrary units (cell index) defined as (Rn−Rb)/15 Ω, with Rn being the impedance at time point n and Rb being the background impedance of wells containing complete growth medium only. Proliferation of cells was calculated as slope of cell index curve per hour.

Enzyme activity of total HDAC

Nuclear extracts of 2102EP and 2102EP-R cells were prepared using the EpiQuik Nuclear Extraction Kit according to the manufacturer's instructions (Epigentek). The protein concentrations

Published OnlineFirst August 24, 2017; DOI: 10.1158/1535-7163.MCT-17-0293

were determined with a BCA Protein Assay Kit (Thermo Fisher Scientific). Enzyme activity was measured with the Epigenase HDAC Activity/Inhibition Direct Assay Kit according to protocol. Briefly, 15 μg of the nuclear extracts were incubated with 0.5 and 1 μmol/L animacroxam or without inhibitor (control) for 90 minutes at 37°C in 96-well plates. Active HDACs bind to the substrate and remove acetyl groups from the substrate. The HDAC-deacetylated products can be recognized with a specific antibody. Finally, solution for color development was added and enzyme activity was measured at 450 nm using an ELISA-Reader (Dynex Technologies). The activity of the total HDAC enzymes is proportional to the OD intensity measured. The experiments were performed three times, and the data are given as mean values ± SD.

Unspecific cytotoxic effects of animacroxam in TGCT cells

Unspecific cytotoxicity of animacroxam on TGCT cell lines was determined on the basis of lactate dehydrogenase (LDH) release from the cytosol of damaged cells (Cytotoxicity Detection Kit, Roche). A total of 4×10^4 cells per well were seeded in 96-well plates for 24 hours at 37°C, 5% CO_2 and then incubated with animacroxam (0.1–10 μmol/L) for 10 hours in culture medium containing 1% FCS. Cells incubated with 1% Triton X-100 served as control for maximum LDH release. The supernatant was transferred to fresh plates and mixed with catalyst and dye solution for 30 minutes, resulting in the formation of formazan dye proportional to enzyme activity. Absorbance was measured at 490/630 nm using an ELISA Reader (Dynex Technologies) and cytotoxicity calculated with untreated cells set at 0% and Triton X-100 lysed cells set at 100%. All experiments were performed in triplicate.

Determination of caspase-3 activity

Preparation of cell lysates and determination of apoptotic caspase- 3 activity was performed as described previously (30). Cleavage of the AC-DEVD-AMC (Calbiochem-Novabiochem) by active caspase-3 resulted in the generation of fluorescent AC-DEVD and was measured with a VersaFluor fluorometer (Bio-Rad; wavelengths: excitation 360 nm, emission 460 nm). Caspase-3 activity is given as the mean ± SD increase in AC-DEVD fluorescence compared with basal activity of untreated controls, which was set to 100%. The experiments were performed $n = 3$.

Cell-cycle analysis by flow cytometry

Cell-cycle distribution was analyzed by flow cytometry of propidium iodide (PI)-stained DNA of treated TGCT cells (31). Cisplatin-sensitive 2102EP, moderately sensitive NCCIT, and cisplatin-resistant 2102EP-R cells were incubated with animacroxam (0.11–0.8 μmol/L), vorinostat (0.7–2.2 μmol/L), or cisplatin (1.4 μmol/L) for 48 hours. PI-stained cellular DNA was analyzed using a BD FACScanto II FACS machine and BD FACSDIVA v6.1.3 software. For each treatment condition, a minimum of 10,000 events per sample were recorded. The experiments were performed $n = 3$.

Western blotting

Western blotting was performed as described before (32). The protein-loaded membranes were incubated with antibodies directed against BAX (1:1,000), BCL-2 (1:1,000; Santa Cruz Biotechnology), CYCLIN D1 (1:200; Sigma-Aldrich), GAPDH (1:5,000; Calbiochem, Merck), and APAF-1 (1:1,000; Cell Signaling Technology). After incubation with horseradish peroxidase–coupled anti-IgG antibodies (1:10,000; Amersham), the blot was developed using the Celvin-S developer (Biostep) and the software SnapAndGo 1.8.1 (Rev.23).

Fluorescence microscopy

Cells were seeded on glass coverslips in 6-well plates (1×10^5 cells/well) and maintained in an incubator for 24 hours at 37°C. Thereafter, cells treated with animacroxam (0.11–2.0 μmol/L) for 3 to 48 hours were washed and fixed for 10 to 15 minutes with 4% paraformaldehyde. After fixation, the cells were washed three times with PBS and blocked with 5% BSA in PBS for 1 hour at room temperature. Then, the cells were washed three times with PBS and incubated with a primary antibody against α-tubulin (1:500; Sigma) at 4°C overnight. After washing with PBS the secondary anti-mouse antibody (1:500; Thermo Fisher Scientific) was applied for 1 hour at room temperature. Cells were then incubated with phalloidin 568 nm (1:200; Invitrogen) for 1 hour at room temperature and DAPI (1:10,000; Merck) for 10 minutes at room temperature. After a final washing step, the coverslips were mounted on glass slides with 10% glycerin in PBS and enclosed with nail polish. Fluorescence microscopy was performed with an Axioskop 40-microscope (Zeiss) at a ×40 magnification. Pictures were taken with a Kappa digital camera system (Kappa Optronics GmbH).

Scratch assay

Scratch assays were performed to investigate animacroxam-induced inhibition of TGCT cell migration. Cells were grown to confluency in a 6-well plate. The cell monolayer was then scratched using a pipet tip. Cells at the edge of this artificial gap migrate into the cell-free area to close the gap in a time-dependent manner. Cisplatin-sensitive 2102EP cells were seeded at a density 1.5×10^5 cells per well and treated with animacroxam (0.22–1 μmol/L) for 24 hours. Changes in the migration of treated cells were determined by comparison and normalization to the migration of the untreated controls using the analysis software TScratch Version 1.0 (CSE Lab). The experiments were performed $n = 3$.

In vivo evaluation of antineoplastic effects of animacroxam

The *in vivo* analysis of the antineoplastic potency of animacroxam was performed using the chorioallantoic membrane assay (CAM assay). This model is an established nonanimal testing method that allows pharmacologic characterization in the living organism but does not require an animal experiment approval. Briefly, fertilized chicken eggs were incubated, and day 1 of incubation is considered the first day of embryonic development. Prior to examination, the eggs were opened and tumors inoculated as described previously (33). Briefly, 1.5×10^6 2102EP cells were resuspended in growth factor–reduced Matrigel (BD Biosciences). The cell suspension was pipetted into a silicone ring (Ø 5 mm), which was placed on the CAM of a 10-day-old fertilized chicken egg and maintained for 48 hours at 37°C to develop microtumors that are attached to the microvasculature of the CAM. Thereafter, the microtumors were topically treated for 96 hours with 20 μl animacroxam (0.8–5 μmol/L). PBS served as the control treatment. Growth of microtumors as well as the viability of the developing embryo was controlled daily by stereomicroscopy using a Kappa digital camera system (Kappa Optronics GmbH).

Safety and tolerability of the novel compound was tested by intravenous injection of animacroxam into a superficial CAM vein at day 11 of chicken embryo development. Twenty microliters

Published OnlineFirst August 24, 2017; DOI: 10.1158/1535-7163.MCT-17-0293

of 0.9% NaCl containing rising concentrations of animacroxam was injected using a 301/2 G needle. Hemorrhage was stopped by applying gentle pressure with a cotton swap for approximately 30 seconds. The effective blood concentration of the injected animacroxam amounted to 0, 2.5, and 5 μmol/L, respectively, assuming a total blood volume of 1 mL of embryo and CAM together for an 11-day-old embryo (34, 35). Chicken embryo development and survival was checked daily for the following 4 days.

Results

Antiproliferative effects of animacroxam in TGCT cells

Three TGCT cell lines with different cisplatin sensitivities (2102EP, sensitive; NCCIT, moderate sensitivity; 2102EP-R, insensitive) were investigated. The IC_{50} values of cisplatin ranged from 1.36 ± 0.12 μmol/L in cisplatin-sensitive 2102EP cells to 5.94 ± 0.5 μmol/L in NCCIT cells, which are regarded as moderately cisplatin sensitive to almost 9 μmol/L in cisplatin-insensitive 2102EP-R cells (Fig. 2D).

Crystal violet staining of animacroxam-treated cells (0.1–3.2 μmol/L) revealed a marked time- and dose-dependent effect on cell survival and decrease in cell number in the three investigated TGCT cell lines. After 96 hours, a drop in cell number of >95% in each cell line (Fig. 2A–C) was observed. The IC_{50} values of animacroxam amounted to 0.22 ± 0.02 μmol/L in cisplatin-sensitive 2102EP cells, 0.42 ± 0.06 μmol/L moderately sensitive NCCIT cells, and 0.30 ± 0.01 μmol/L in cisplatin-resistant 2102EP-R cells (Fig. 2D), showing that animacroxam-induced growth inhibition of TGCT cells occurs at nanomolar concentrations, independently of the level of cisplatin sensitivity. The growth-inhibitory effects of the approved HDAC inhibitor vorinostat were less pronounced with IC_{50} doses of 1.43 ± 0.22 μmol/L (2102EP), 1.73 ± 0.13 μmol/L (NCCIT), and 2.22 ± 0.3 μmol/L (2102EP-R), respectively (Fig. 2D).

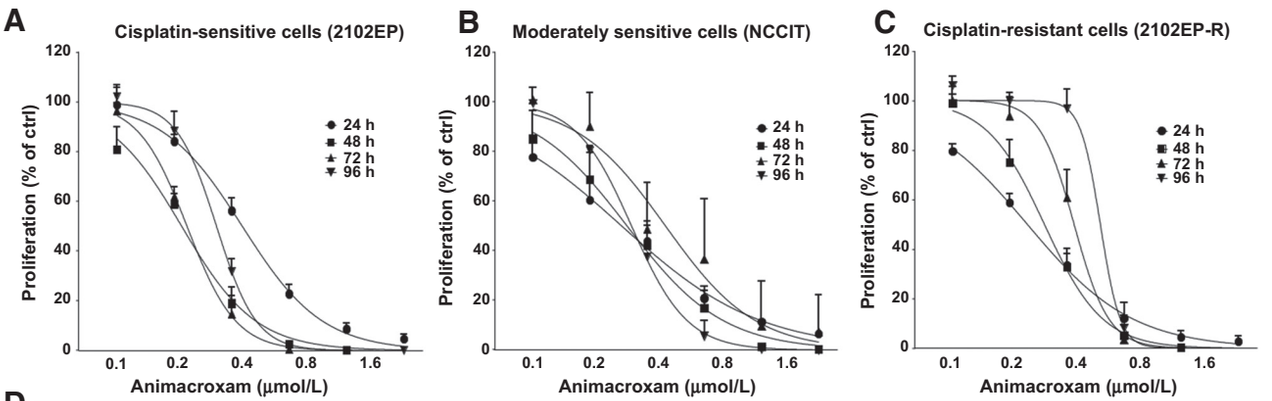

D

Cell line	Animacroxam	Vorinostat	Cisplatin
Cisplatin-sensitive cells (2102EP)	0.22 ± 0.02 μmol/L	1.43 ± 0.22 μmol/L	1.36 ± 0.12 μmol/L
Moderately sensitive cells (NCCIT)	0.42 ± 0.06 μmol/L	1.73 ± 0.13 μmol/L	5.94 ± 0.50 μmol/L
Cisplatin-resistant cells (2102EP-R)	0.30 ± 0.01 μmol/L	2.22 ± 0.30 μmol/L	8.96 ± 0.87 μmol/L

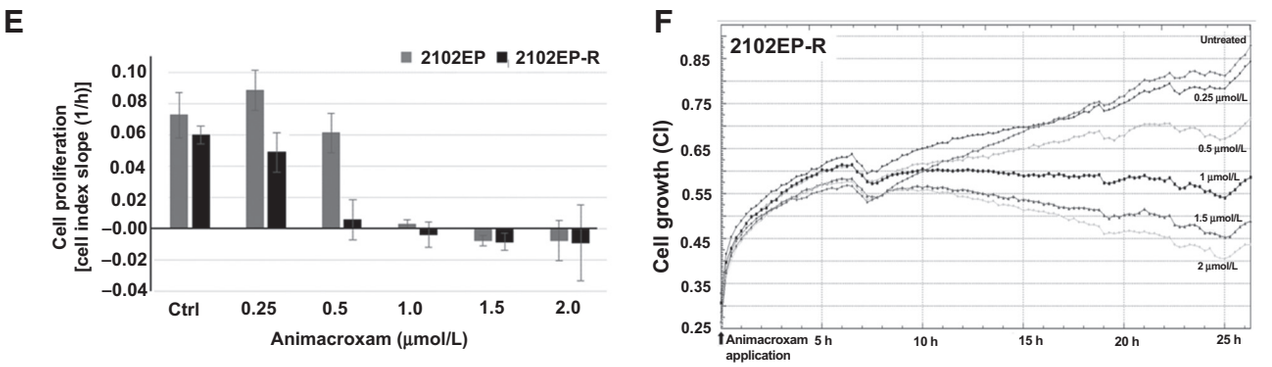

Figure 2.

Growth inhibition of TGCT cell animacroxam and half-maximal concentrations. Crystal violet staining was employed to determine the time- and dose-dependent antiproliferative effects of animacroxam (0.1–3.2 μmol/L) in cisplatin-sensitive cells (**A**; 2102EP), moderately sensitive cells (**B**; NCCIT), and cisplatin-resistant cells (**C**; 2102EP-R). **D,** Determination of IC_{50} values of animacroxam, vorinostat, and cisplatin in TGCT cells after 48 hours of incubation. **E,** Real-time proliferation of cisplatin-sensitive and resistant cells after treatment with increasing concentrations of animacroxam measured with iCELLigence system. Time course of proliferation was reflected in the slope of the curves and was calculated as means ± SD. **F,** Dose-dependent effects of animacroxam on the cell index curves of 2102EP-R cells within the first 25 hours of incubation. All results are described as means ± SD of 3 to 4 independent experiments.

Published OnlineFirst August 24, 2017; DOI: 10.1158/1535-7163.MCT-17-0293

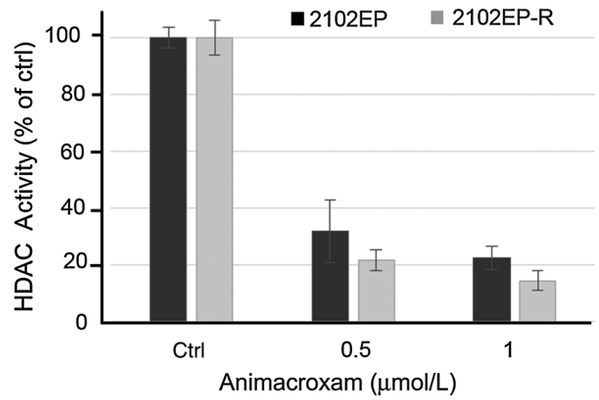

Figure 3.
Inhibition of HDAC enzyme activity by animacroxam. Total HDAC enzyme activity was measured in 15 μg nuclear extracts of 2102EP and 2102EP-R cells after incubation with 0.5 or 1 μmol/L animacroxam for 90 minutes. Enzyme activity is given relative to untreated control extracts as means ± SD of $n = 3$ independent experiments.

Real-time monitoring of cell proliferation

Changes in the proliferation rates of animacroxam-treated TGCT cells were determined in real time by using the noninvasive iCELLigence system for 72 hours in 15-minute intervals. Cell index calculations served as an indicator of cell proliferation and showed a marked reduction of TGCT cell growth at 0.5 μmol/L (2102EP-R) or 1 μmol/L (2102EP), respectively, as depicted in Fig. 2E. NCCIT cells treated with animacroxam showed a profile comparable with that of treated 2102EP cells. IC_{50} values calculated after 48 hours amounted to 0.6 μmol/L for 2102EP and 0.33 μmol/L for 2102EP-R, verifying the crystal violet staining data. Furthermore, the continuous monitoring also revealed that the onset of the animacroxam-induced growth inhibition occurred after 10 hours (Fig. 2F).

Inhibition of HDAC enzyme activity

To verify the HDAC inhibitory effectiveness of animacroxam, nuclear extracts of cisplatin-sensitive 2102EP and cisplatin-resistant 2102EP cells were incubated with 0.5 or 1 μmol/L animacroxam, and the inhibition of total HDAC enzyme activity was measured using the Epigenase HDAC Enzyme Activity Kit. Pan-HDAC activity was reduced by up to 80% in 2102EP and up to 85% in the cisplatin-resistant 2102EP-R cells (Fig. 3), confirming the HDAC-inhibitory potency of the hydroxamic acid moiety of animacroxam.

Unspecific cytotoxicity of animacroxam

TGCT cell lines were also checked for unspecific cytotoxic effects after 10 hours of incubation with 0.1 to 10 μmol/L animacroxam by measuring the release of LDH from damaged cells into the supernatant of the culture medium. However, no increased LDH release was observed at nanomolar animacroxam concentrations that were shown to be effective in inhibiting cell growth (Fig. 4). Even at its maximum dose of 10 μmol/L, animacroxam gave rise to only a marginal increase in unspecific cytotoxicity of approximately 3%, indicating that the mode of action of animacroxam is not based on the induction of unspecific cell damage.

Regulation of apoptosis by animacroxam

Treatment of TGCT cells with animacroxam (0.1–2.0 μmol/L) led to a dose-dependent increase in caspase-3 activity after 48 hours, for example, to an approximately 14-fold increase in cisplatin-sensitive 2102EP cells relative to untreated control cells. In NCCIT cells, the caspase-3 activity rose 9-fold, and in cisplatin-resistant 2102EP-R cells, animacroxam induced a hike in caspase-3 activity by a factor of 16.5 (Fig. 5A).

Treatment with vorinostat (0.2–2 μmol/L) led to a comparable rise in caspase-3 activities (Fig. 5B). To further elucidate animacroxam-induced apoptosis, the expression levels of the pro- and antiapoptotic proteins BAX and BCL-2, as well as of APAF-1, were investigated by Western blot analysis. Interestingly, Western blot assays revealed that the protein expression ratio of BCL-2/BAX differed for the two cell lines 2102EP and 2102EP-R. Specifically, animacroxam was able to attenuate the expression of BCL-2 while not enhancing the expression of BAX in the cisplatin-sensitive cell model 2102EP upon 12 hours of treatment (Fig. 5C). In contrast, in the cisplatin-resistant 2102EP-R cells, the expression levels of BCL-2 and BAX were not significantly altered after animacroxam treatment (Fig. 5D). In both cell models, the expression level of the proapoptotic protein APAF-1 was significantly upregulated even after short periods of incubation (6 hours), indicating a mitochondria-driven apoptosis induction. As seen already in the

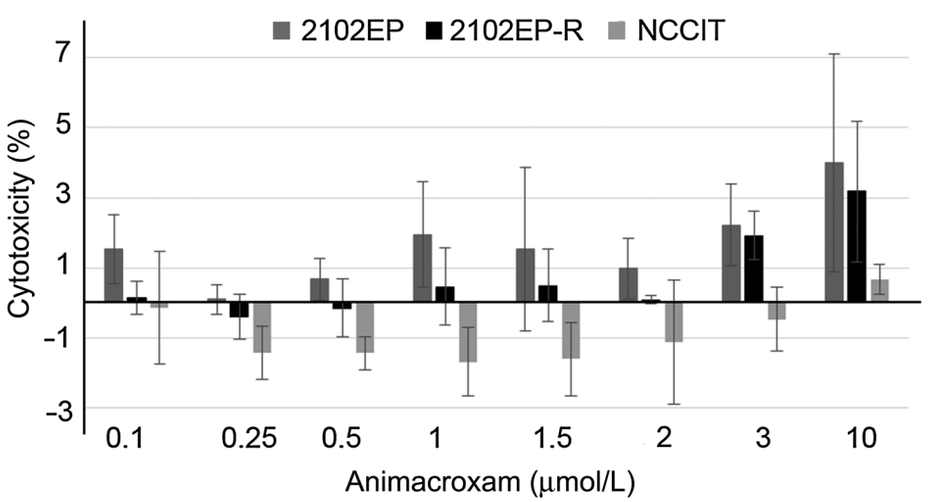

Figure 4.
Unspecific cytotoxic effects of animacroxam in TGCT. LDH release of 2102EP, 2102EP-R, and NCCIT cells was measured after 10 hours of incubation with 0.1 to 10 μmol/L animacroxam. Results show changes in LDH release as compared with untreated cells. Data are given as percentage changes of basal LDH release of controls. Means ± SD of $n = 3$ independent experiments.

Published OnlineFirst August 24, 2017; DOI: 10.1158/1535-7163.MCT-17-0293

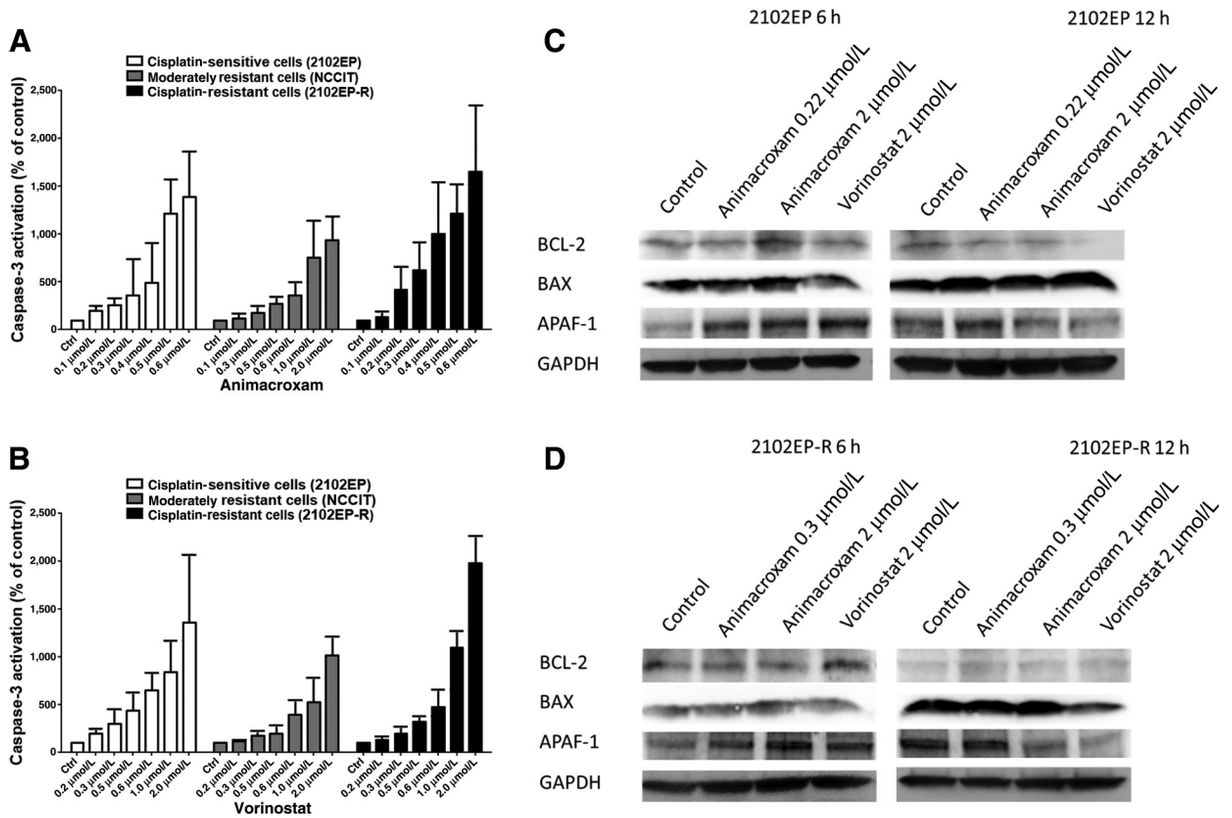

Figure 5.

Apoptotic effects of animacroxam in TGCT cells. **A,** Caspase-3 activation in cisplatin-sensitive 2102EP cells, moderately sensitive NCCIT cells, and cisplatin-resistant 2102EP-R cells after treatment with increasing concentrations of animacroxam (0.1–2.0 µmol/L) for 48 hours. **B,** Caspase-3 activation in 2102EP, NCCIT, and 2102EP-R cells after treatment with increasing concentrations of vorinostat (0.2–2.0 µmol/L) for 48 hours. Results are given as means ± SD of $n = 3$ independent experiments. **C** and **D,** Representative Western blots showing animacroxam induced changes in the expression of anti-apoptotic BCL-2, pro-apoptotic BAX, and the mitochondrial mediator of apoptosis APAF-1 after 6 and 12 hours of incubation with animacroxam and vorinostat, respectively.

caspase-3 activity assay, vorinostat treatment led to similar effects on the levels of apoptosis-related proteins in both cell lines.

Influence of animacroxam on cell-cycle regulation of TGCT

Cell cycle–modulating effects of animacroxam in cisplatin-sensitive and resistant cells were investigated by flow cytometry. After 48 hours of incubation with animacroxam (0.11–0.8 µmol/L), a dose-dependent arrest of TGCT cells in the G_0–G_1-phase of the cell cycle and a concomitant decrease in the G_2–M-phase population was observed (Fig. 6A–C). The cell-cycle arresting effect of animacroxam was independent of the cisplatin sensitivity of the cells. In contrast, vorinostat exhibited only marginal cell-cycle arresting effects in 2012EP and 2102EP-R cells. However, in NCCIT cells, the cell-cycle arresting effects of vorinostat were as pronounced as those of animacroxam.

To further elucidate the molecular mechanism of the G_0–G_1-phase arresting effects of animacroxam, the expression of the cell-cycle promotor CYCLIN D1, which acts at the transition from the G_1 to S phase, was examined at two different time points. Animacroxam treatment (2.0 µmol/L) caused a slight downregulation of cyclin D1 in cisplatin-sensitive cells after 12 hours of incubation but not in the cisplatin-resistant 2102EP cells (Fig. 6D). In the moderately sensitive NCCIT cells, CYCLIN D1 was upregulated until 24 hours of incubation with animacroxam. The positive control vorinostat did not enhance the expression of Cyclin D1 in the 2102EP and 2102EP-R cells. Only in the moderately sensitive cell line NCCIT, vorinostat induced an increase in CYCLIN D1 expression after 24 hours, confirming the findings observed by flow cytometry analysis.

Cytoskeletal alterations by animacroxam

The effect of animacroxam on the cytoskeleton was investigated in cisplatin-sensitive 2102EP cells. Incubation with animacroxam (0.22 or 2 µmol/L) for 48 hours led to actin stress fiber formation, while the architecture of tubulin structures was not affected (Fig. 7A–C). The occurrence of actin stress fibers was time dependent and was not observed until 24 hours of incubation. In contrast, no actin stress fiber formation was observed upon incubation with vorinostat (2 µmol/L) for up to 48 hours, underlining the pleiotropic mode of action of animacroxam as compared with the merely HDAC-inhibitory effect of vorinostat.

Influence of animacroxam on the migration of TGCT cells

As cytoskeletal alterations strongly influence the plasticity and the migratory propensity of tumor cells, so-called "wound healing" assays were performed. These assays allow ascertaining the potential of tumor cells to fill a gap in the cell monolayer created

Published OnlineFirst August 24, 2017; DOI: 10.1158/1535-7163.MCT-17-0293

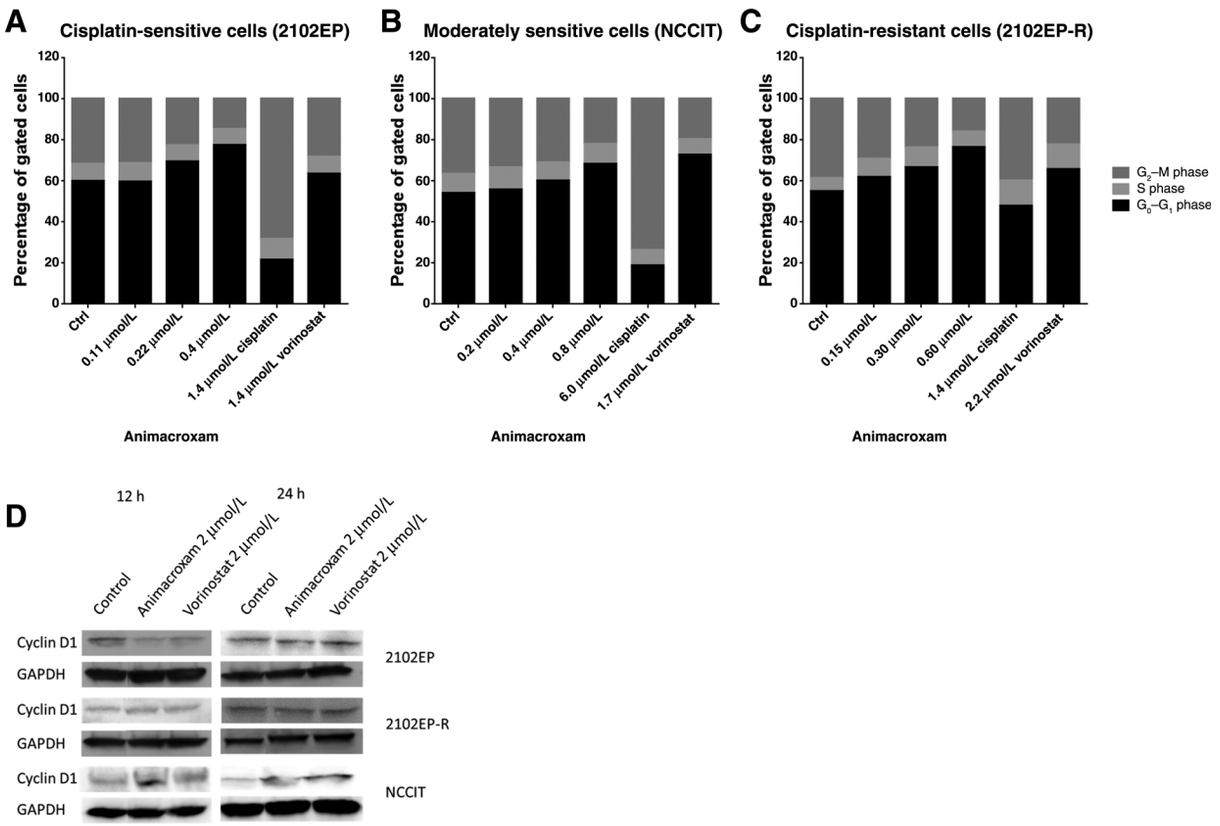

Figure 6.

Influence of animacroxam on the cell cycle of TGCT. Animacroxam induced a cell-cycle arrest in the G_0–G_1 phase of cisplatin-sensitive 2102EP cells (**A**), moderately sensitive NCCIT cells (**B**), and cisplatin-resistant 2102EP-R cells (**C**) after 48 hours of incubation. Data are given as percentage of untreated controls (means of $n = 3$ independent experiments). **D,** Representative Western blots of animacroxam and vorinostat induced changes in the expression of the cell-cycle promotor CYCLIN D1 in TGCT cells.

by scratching, not by proliferation but by active migration. They revealed that untreated control cells reduced the scratch area by 23.5% after 24 hours (Fig. 7D and E), while 2102EP cells treated with animacroxam (0.22 µmol/L) closed the scratch by only 18.8%. When applied at higher concentrations, animacroxam (1.0 µmol/L) almost completely inhibited cell migration to the effect of a reduction of the scratch area of only 4% after 24 hours.

In vivo evaluation of animacroxam

Using the CAM assay, the effects of animacroxam on TGCT tumor growth were evaluated *in vivo*. Microtumors of 2102EP cells were inoculated onto the CAM of 10-day-old chicken embryos, and after connection to the microvasculature of the CAM, the tumors were treated with animacroxam for up to 96 hours. Animacroxam treatment led to a dose- and time-dependent inhibition of tumor growth, as compared with the untreated controls, which steadily increased in size and volume (Fig. 8).

Tolerability and safety of animacroxam *in vivo*

Embryo toxicity in terms of regular development and lethality was evaluated by intravenous injections with increasing concentrations of animacroxam (0–5 µmol/L). Injections were performed on 11-day-old chicken embryos, and survivability was followed for 4 days. Animacroxam was well tolerated, and even at concentrations as high as 5 µmol/L, no increased lethality was observed when compared with untreated controls. Embryo development appeared to be age based and did not differ from those of untreated controls. All chicken embryos were sacrificed at the end of the study and examined for developmental defects, such as encephalic hernia or cleft beak (36). However, no such defects were found in animacroxam-injected embryos, further supporting the good tolerability of the novel compound.

Discussion

Malignant germ cell tumors of the testis are the most common solid tumors in males under 50 years of age. Although the general platinum-based chemotherapy is very effective, it also implies severe risks and drawbacks, such as the occurrence of early and late toxicities, primary and secondary platinum resistances, or a higher incidence of secondary malignancies. Moreover, high requirements are to be met (general good condition, good renal functioning, etc.) by patients to qualify for a platinum-based chemotherapy.

Thus, a key challenge in an alternative treatment of recurrent germ cell tumors is to overcome the aforementioned difficulties that may occur under the currently used second-line salvage treatment with a platinum-based high-dose combination

Published OnlineFirst August 24, 2017; DOI: 10.1158/1535-7163.MCT-17-0293

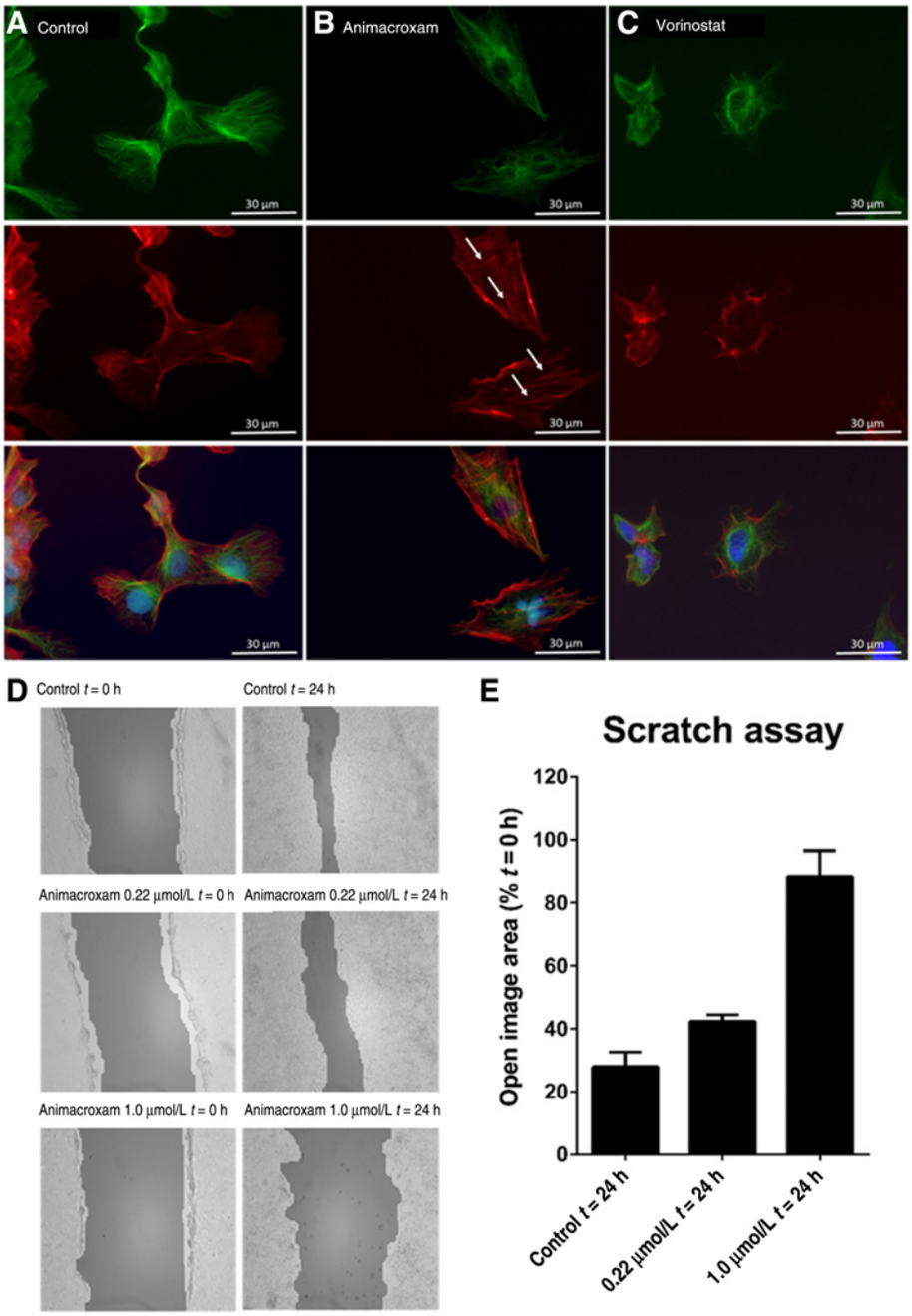

Figure 7.
Cytoskeletal alterations and antimigratory effects of animacroxam. In contrast to vorinostat, animacroxam induced the formation of f-actin stress fibers in cisplatin-sensitive TGCT cells, as indicated by arrows. **A,** Untreated control, **B,** Treatment (48 hours) with animacroxam (0.22 μmol/L). **C,** Treatment (48 hours) with vorinostat (1.5 μmol/L). Green, α-tubulin; red, f-actin; blue, DAPI. Magnification, ×40. **D,** Representative images of antimigratory effects of animacroxam analyzed by scratch assays. Incubation for 24 hours with animacroxam (0.22 and 1.0 μmol/L) resulted in a reduced migration of cisplatin-sensitive 2102EP cells as shown by a repressed closure of the open image area. **E,** Quantification of the open image area (in %) after 0 and 24 hours of incubation with animacroxam. Results are given as means ± SD of $n = 3$ independent experiments.

regimen (37, 38). Recently, we introduced conjugates of hydroxamic acids and imidazoles as promising new dual-mode compounds for cancer treatment. They combine HDAC inhibition with cytoskeleton modulation, causing a strong overall cell growth–inhibitory effect, as recently shown by us for several non-TGCT cancer cell lines (27). Herein, we investigated animacroxam, one of the most efficacious compounds of this series, for its antitumor effects on TGCT cells with different platinum sensitivities.

We demonstrated that animacroxam exerts a strong antiproliferative effect at nanomolar concentrations in TGCT cells, regardless of their cisplatin sensitivity. This growth-inhibitory effect occurred 10 hours postincubation and at significantly lower doses when compared with the clinically established HDACi vorinostat (39). The antitumor effects of animacroxam were found to originate from a strong inhibition of HDAC enzyme activity and specific alterations in signaling pathways connected to apoptosis and cell-cycle regulation, but were not based on unspecific cytotoxicity of the compound. The remaining approximately 15% of HDAC activity in TGCT (see Fig. 3) occurred due to an incomplete pan-HDAC inhibition at the given concentrations, but may also reflect a subtype-specific inhibition of the majority of HDACs, but not of all. This open question needs further clarification in coming experiments, as it is valuable information for predicting the

Published OnlineFirst August 24, 2017; DOI: 10.1158/1535-7163.MCT-17-0293

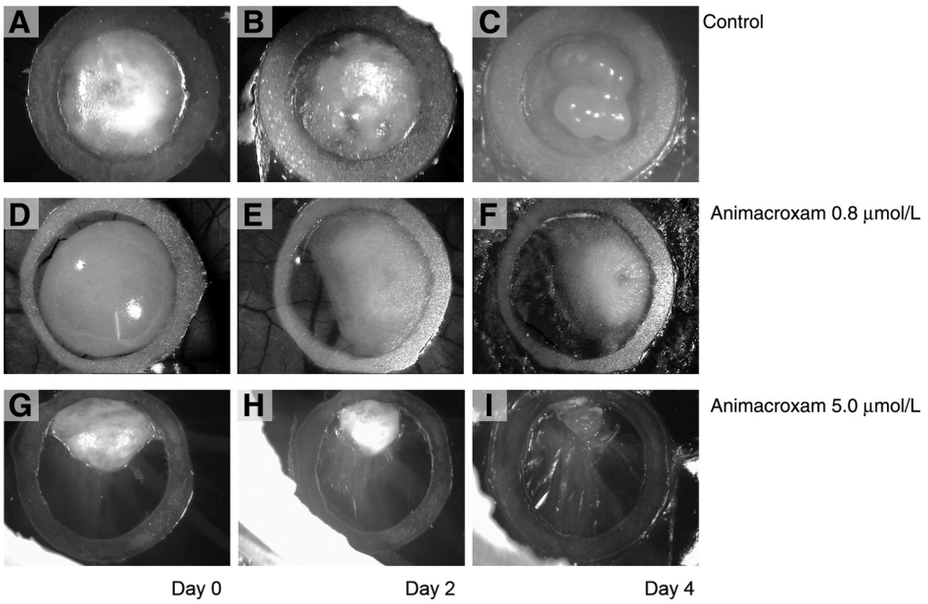

Figure 8.
Antineoplastic effects of animacroxam *in vivo*. TGCT microtumors inoculated onto the CAM of fertilized chicken eggs showed a time- and dose-dependent reduction in tumor size and volume after animacroxam treatment. In contrast, NaCl (0.9%) treated control tumors time dependently increased in size and volume. **A–C,** NaCl-treated microtumor at the beginning of the treatment (**A**), after 2 days (**B**), and after 4 days (**C**). **D–I,** Animacroxam-treated microtumors (0.8 and 5 µmol/L) at the beginning of the treatment (**D**; **G**), after 2 days (**E**; **H**), and after 4 days (**F**; **I**). Representative findings of $n = 3$ independent preparations for each concentration.

efficacy of the novel compound in different tumor entities with different HDAC expression patterns.

Animacroxam caused a pronounced increase in apoptosis-specific caspase-3 activity in TGCT cells. This is in line with earlier findings that showed that animacroxam can induce apoptosis in certain human melanoma cells (40). The extent of caspase-3 induction by 0.6 µmol/L animacroxam exceeded by far a similar effect of vorinostat, again regardless of the cisplatin sensitivity of the investigated cell lines. The downregulation of BCL-2 after 12 hours of incubation in the cisplatin-sensitive 2102EP cells shows that animacroxam inhibits antiapoptotic signaling, resulting in an increased caspase-3 activation. BAX levels were not affected. This is in line with the observed caspase-3 activation and induction of cell death. APAF-1 was upregulated early on in both the cisplatin-sensitive and resistant 2102EP cells. This fact corroborated the assumption of a mitochondria-mediated apoptosis induction.

Flow cytometric analysis of animacroxam-treated TGCT cells showed a dose-dependent G_0–G_1-phase arrest in all investigated TGCT cell lines, again independent of their cisplatin sensitivity. CYCLIN D1 is required for progression through the G_1 phase of the cell cycle, and it regulates the transition and entry into the S-phase by binding to cyclin-dependent kinases 4 and 6 (Cdk4/6). CYCLIN D1 is often overexpressed in cancer and is associated with early cancer onset and tumor progression (41).

After 12 hours of incubation, animacroxam induced a down-regulation of CYCLIN D1 and thereby the accumulation of cisplatin-sensitive 2102EP cells in G_1-phase. This effect of animacroxam fits in with the observed G_0–G_1-phase arrest and indicates that the new compound acts on this crucial regulator of cell-cycle progression, which is known to be dysregulated in TGCT and whose repression has already been suggested as a molecular target for germ cell tumors (42). Interestingly and contrary to the FACS analysis, this effect was not observed in cisplatin-resistant 2102EP-R cells. These findings suggest that animacroxam might be applied as a component of a combination regimen with chemotherapeutic agents that act in different or several phases of the cell cycle, thus enabling additive or synergistic effects. Potential combination drugs are bleomycin, a proven antitumor antibiotic, etoposide, a well-established topoisomerase II inhibitor (43), or anthracyclines such as doxorubicin, which is widely used in combination therapy (44).

Next, we investigated the effects of animacroxam on the cytoskeletal organization of the TGCT cells. It was found earlier that aptly substituted 4,5-diarylimidazoles disrupt the cytoskeleton preferentially of cancer cells (45), and induce the formation of actin stress fibers in HUVEC cells (46). As a consequence, these cell structures likely lack the normal dynamic cytoskeletal turnover, which is essential for active proliferation and migration (47). Exemplarily, we investigated cisplatin-sensitive 2102EP cells for changes of their cytoskeletal organization upon animacroxam treatment. In accordance with recent findings on human HUVEC cells, we could show that animacroxam induces the formation of actin stress fibers in TGCT cells after 48 hours of incubation. These cytoskeletal effects also explain the higher sensitivity of TGCT of animacroxam, when compared with the HDAC inhibitor vorinostat, which does not interfere with the integrity or dynamics of the actin cytoskeleton.

The loss of cytoskeletal plasticity and dynamics, which are thought to be responsible for the loss of cancer cell motility (48), was investigated by scratch assays. Animacroxam (0.22–1.0 µmol/L) led to a reduction of TGCT cell migration of up to 96%. When treated with 1.0 µmol/L animacroxam, TGCT cells showed virtually no migration anymore and even started to detach from the surface, which is an indication for the loss of the adhesive capacity of their cytoskeleton. Migration of tumor cells is characterized by the formation of finger-like projections called filopodia (49), which were absent in treated TGCT cells as depicted in the microscopy images. This underlines that cancer cell migration, and hence aggressiveness and metastasizing, is effectively inhibited or at least attenuated by the pleiotropic agent animacroxam.

The CAM assay is an established (xenograft) model for the *in vivo* testing of antineoplastic compounds (50–52). Moreover, it is an easy method to check for toxic effects of experimental compounds *in vivo*, as it can be injected into the embryo-feeding CAM, and the development and survival of the chicken embryo can be

evaluated in the following days. Establishing TGCT microtumors, which got connected to the microvasculature of the CAM of fertilized chicken eggs, we could show that the treatment with animacroxam reduced TGCT tumor growth *in vivo* time- and dose dependently, thus confirming the pronounced antiproliferative and apoptosis-inducing effects seen in our *in vitro* experiments.

Moreover, investigations on possible toxic effects of animacroxam in the fragile and sensitive chicken embryos revealed that the compound was very well tolerated and did not induce embryo toxicity or developmental delays. Even at a very high concentration of 5 μmol/L, which was maximally effective in reducing TGCT tumor growth, there was no increased lethality.

In the current work, we could demonstrate the growth-inhibitory, apoptosis-inducing, cell-cycle arresting, and cytoskeleton-disrupting effects of the novel dual-mode inhibitor animacroxam in TGCT cells, regardless of their cisplatin sensitivity. Moreover, the compound showed pronounced antineoplastic potency and excellent tolerability *in vivo*. The results indicate that animacroxam may be a promising lead compound for the development of novel drugs that could complement the platinum-based chemotherapy that is generally used for TGCT today.

Disclosure of Potential Conflicts of Interest

No potential conflicts of interest were disclosed.

Authors' Contributions

Conception and design: G. Steinemann, B. Nitzsche, M. Höpfner
Development of methodology: G. Steinemann, A. Dittmer, B. Nitzsche, M. Höpfner
Acquisition of data (provided animals, acquired and managed patients, provided facilities, etc.): G. Steinemann, A. Dittmer, W. Kuzyniak, R. Schobert, B. Biersack, B. Nitzsche, M. Höpfner
Analysis and interpretation of data (e.g., statistical analysis, biostatistics, computational analysis): G. Steinemann, A. Dittmer, B. Nitzsche, M. Höpfner
Writing, review, and/or revision of the manuscript: G. Steinemann, A. Dittmer, W. Kuzyniak, B. Hoffmann, R. Schobert, B. Biersack, B. Nitzsche, M. Höpfner
Administrative, technical, or material support (i.e., reporting or organizing data, constructing databases): G. Steinemann, W. Kuzyniak, B. Hoffmann, M. Schrader, B. Nitzsche, M. Höpfner
Study supervision: M. Höpfner

Grant Support

G. Steinemann was funded by the Fazit-Stiftung and the Ruth-Jeschke-Gedenkstipendium awarded by the Charité Berlin. A. Dittmer was funded by the Else Kröner-Fresenius-Stiftung.

The costs of publication of this article were defrayed in part by the payment of page charges. This article must therefore be hereby marked *advertisement* in accordance with 18 U.S.C. Section 1734 solely to indicate this fact.

Received April 3, 2017; revised July 26, 2017; accepted August 9, 2017; published OnlineFirst August 24, 2017.

References

1. Chia VM, Quraishi SM, Devesa SS, Purdue MP, Cook MB, McGlynn KA. International trends in the incidence of testicular cancer, 1973-2002. Cancer Epidemiol Biomarkers Prev 2010;19:1151–9.
2. Feldman DR, Bosl GJ, Sheinfeld J, Motzer RJ. Medical treatment of advanced testicular cancer. JAMA 2016;299:672–84.
3. Oechsle K, Kollmannsberger C, Honecker F, Mayer F, Waller CF, Hartmann JT, et al. Long-term survival after treatment with gemcitabine and oxaliplatin with and without paclitaxel plus secondary surgery in patients with cisplatin-refractory and/or multiply relapsed germ cell tumors. Eur Urol 2011;60:850–5.
4. Mueller T, Mueller LP, Holzhausen H, Witthuhn R, Albers P, Schmoll H-J. Histological evidence for the existence of germ cell tumor cells showing embryonal carcinoma morphology but lacking OCT4 expression and cisplatin sensitivity. Histochem Cell Biol 2010;134:197–204.
5. van Schinkel LD, Willemse PM, van der Meer RW, Burggraaf J, van Elderen SGC, Smit JWA, et al. Chemotherapy for testicular cancer induces acute alterations in diastolic heart function. Br J Cancer 2013;109:891–6.
6. Brydøy M, Oldenburg J, Klepp O, Bremnes RM, Wist EA, Wentzel-Larsen T, et al. Observational study of prevalence of long-term Raynaud-like phenomena and neurological side effects in testicular cancer survivors. J Nat Cancer Inst 2009;101:1682–95.
7. Haugnes HS, Bosl GJ, Boer H, Gietema JA, Brydøy M, Oldenburg J, et al. Long-term and late effects of germ cell testicular cancer treatment and implications for follow-up. J Clin Oncol 2012;30:3752–63.
8. Fung C, Fossa SD, Milano MT, Oldenburg J, Travis LB. Solid tumors after chemotherapy or surgery for testicular nonseminoma: a population-based study. J Clin Oncol 2013;31:3807–14.
9. Allfrey VG, Faulkner R, Mirsky AE. Acetylation and methylation of histones and their possible role in the regulation of RNA synthesis. Proc Natl Acad Sci U S A 2016;51:786–94.
10. Bird A. DNA methylation patterns and epigenetic memory. Genes Dev 2002;16:6–21.
11. Jones DO, Cowell IG, Singh PB. Mammalian chromodomain proteins: their role in genome organisation and expression. BioEssays 2000;22:124–37.
12. Hongs L, Schrothp GP, Matthew HR, Yaus P, Bradburysliii EM. Studies of the DNA binding properties of histone H4 amino terminus. J Biol Chem 1993;268:305–14.
13. Khan O, La Thangue NB. HDAC inhibitors in cancer biology: emerging mechanisms and clinical applications. Immunol Cell Biol 2012;90:85–94.
14. Krusche CA, Wülfing P, Kersting C, Vloet A, Böcker W, Kiesel L, et al. Histone deacetylase-1 and -3 protein expression in human breast cancer: a tissue microarray analysis. Breast Cancer Res Treat 2005;90:15–23.
15. Weichert W, Röske A, Gekeler V, Beckers T, Stephan C, Jung K, et al. Histone deacetylases 1, 2 and 3 are highly expressed in prostate cancer and HDAC2 expression is associated with shorter PSA relapse time after radical prostatectomy. Br J Cancer 2008;98:604–10.
16. Fritzsche FR, Weichert W, Röske A, Gekeler V, Beckers T, Stephan C, et al. Class I histone deacetylases 1, 2 and 3 are highly expressed in renal cell cancer. BMC Cancer 2008;8:381.
17. He L, Tolentino T, Grayson P, Zhong S, Warrell RP, Rifkind RA, et al. Histone deacetylase inhibitors induce remission in transgenic models of therapy-resistant acute promyelocytic leukemia. J Clin Invest 2001;108:1321–30.
18. Grignani F, De Matteis S, Nervi C, Tomassoni L, Gelmetti V, Cioce M, et al. Fusion proteins of the retinoic acid receptor-alpha recruit histone deacetylase in promyelocytic leukaemia. Nature 1998;391:815–8.
19. Lin RJ, Nagy L, Inoue S, Shao W, Miller WH, Evans RM. Role of the histone deacetylase complex in acute promyelocytic leukaemia. Nature 1998;391:811–4.
20. Einhorn LH, Donohue J. Cis-Diamminedichloroplatinum, vinblastine, and bleomycin combination chemotherapy in disseminated testicular cancer. Ann Intern Med 1997;87:293–8.
21. Schobert R, Biersack B. Multimodal HDAC inhibitors with improved anticancer activity. Curr Cancer Drug Targets 2017 Feb 5. [Epub ahead of print].
22. Whittaker SJ, Demierre M-F, Kim EJ, Rook AH, Lerner A, Duvic M, et al. Final results from a multicenter, international, pivotal study of romidepsin in refractory cutaneous T-cell lymphoma. J Clin Oncol 2010;28:4485–91.
23. Butler LM, Zhou X, Xu W, Scher HI, Rifkind RA, Marks PA, et al. The histone deacetylase inhibitor SAHA arrests cancer cell growth, up-regulates thioredoxin-binding protein-2, and down-regulates thioredoxin. Proc Natl Acad Sci U S A 2014;99:11700–5.
24. Schobert R, Biersack B, Dietrich A, Effenberger K, Knauer S, Mueller T. 4-(3-Halo/amino-4,5-dimethoxyphenyl)-5-aryloxazoles and -N-methylimidazoles that are cytotoxic against combretastatin A resistant tumor cells and

Published OnlineFirst August 24, 2017; DOI: 10.1158/1535-7163.MCT-17-0293

vascular disrupting in a cisplatin resistant germ cell tumor model. J Med Chem 2010;53:6595–602.
25. Barr MP, Gray SG, Hoffmann AC, Hilger RA, Thomale J, O'Flaherty JD, et al. Generation and characterisation of cisplatin-resistant non-small cell lung cancer cell lines displaying a stem-like signature. PLoS One 2013;8:e54193.
26. Sheikine Y, Genega E, Melamed J, Lee P, Reuter VE, Ye H. Molecular genetics of testicular germ cell tumors. Am J Cancer Res 2012;2:153–67.
27. Mahal K, Schruefer S, Steinemann G, Rausch F, Schobert R, Biersack B, et al. Biological evaluation of 4,5-diarylimidazoles with hydroxamic acid appendages as novel dual mode anticancer agents. Cancer Chemother Pharmacol 2015;75:691–700.
28. Steinemann G, Jacobsen C, Gerwing M, Hauschild J, von Amsberg G, Höpfner M, et al. Activity of nintedanib in germ cell tumors. Anticancer Drugs 2016;27:89–98.
29. Nitzsche B, Gloesenkamp C, Schrader M, Ocker M, Preissner R, Lein M, et al. Novel compounds with antiangiogenic and antiproliferative potency for growth control of testicular germ cell tumours. Br J Cancer 2010;103:18–28.
30. Gloesenkamp C, Nitzsche B, Lim AR, Normant E, Vosburgh E, Schrader M, et al. Heat shock protein 90 is a promising target for effective growth inhibition of gastrointestinal neuroendocrine tumors. Int J Oncol 2012;40:1659–67.
31. Maaser K, Höpfner M, Jansen A, Weisinger G, Gavish M, Kozikowski AP, et al. Specific ligands of the peripheral benzodiazepine receptor induce apoptosis and cell cycle arrest in human colorectal cancer cells. Br J Cancer 2001;85:1771–80.
32. Höpfner M, Sutter AP, Huether A, Schuppan D, Zeitz M, Scherübl H. Targeting the epidermal growth factor receptor by gefitinib for treatment of hepatocellular carcinoma. J Hepatol 2004;41:1008–16.
33. Nitzsche B, Gloesenkamp C, Schrader M, Hoffmann B, Zengerling F, Balabanov S, et al. Anti-tumour activity of two novel compounds in cisplatin-resistant testicular germ cell cancer. Br J Cancer 2012;107: 1853–63.
34. Kind C. The development of the circulating blood volume of the chick embryo. Anat Embryol 1975;147:127–32.
35. Barnes A, Jensen W. Blood volume and the red cel concentrationin the normal chick embryo. Am J Physiol 1959;197:403–5.
36. Peterka M, Klepa I. Light irradiation increases embryotoxicity of photodynamic therapy sensitizers (5-aminolevulinic acid and protoporphyrin IX) in chick embryos. Reprod Toxicol 2001;15:111–6.
37. Lorch A, Kollmannsberger C, Hartmann JT, Metzner B, Schmidt-wolf IGH, Berdel WE, et al. Single versus sequential high-dose chemotherapy in patients with relapsed or refractory germ cell tumors: a prospective randomized multicenter trial of the german testicular cancer study group. J Clin Oncol 2007;25:2778–84.
38. Schrader M, Kempkensteffen C, Christoph F, Hinz S, Weikert S, Lein M, et al. Germ cell tumors of the gonads: a selective review emphasizing problems in drug resistance. Oncology 2009;76:77–84.
39. Millward M, Price T, Townsend A, Sweeney C, Spencer A, Sukumaran S, et al. Phase 1 clinical trial of the novel proteasome inhibitor marizomib with the histone deacetylase inhibitor vorinostat in patients with melanoma, pancreatic and lung cancer based on in vitro assessments of the combination. Invest New Drugs 2012;30: 2303–17.
40. Mahal K, Kahlen P, Biersack B, Schobert R. 4-(1-Ethyl-4-anisyl-imidazol-5-yl)-N-hydroxycinnamide - A new pleiotropic HDAC inhibitor targeting cancer cell signalling and cytoskeletal organisation. Exp Cell Res 2015;336:263–75.
41. Diehl JA. Cycling to cancer with cyclin D1. Cancer Biol Ther 2002;1:226–31.
42. Freemantle SJ, Vaseva AV, Ewings KE, Bee T, Krizan KA, Kelley MR, et al. Repression of cyclin D1 as a target for germ cell tumors. Int J Oncol 2007;30:333–40.
43. Homesley HD, Bundy BN, Hurteau JA, Roth LM. Bleomycin, etoposide, and cisplatin combination therapy of ovarian granulosa cell tumors and other stromal malignancies. Gynecol Oncol 1999;72:131–7.
44. Intergroup A, Trial E, Sledge BGW, Neuberg D, Bernardo P, Ingle JN, et al. Combination of doxorubicin and paclitaxel as front-line chemotherapy for metastatic breast Cancer2017;21:588–92.
45. Bonezzi K, Taraboletti G, Borsotti P, Bellina F, Rossi R, Giavazzi R. Vascular disrupting activity of tubulin-binding 1,5-diaryl-1H-imidazoles. J Med Chem 2009;52:7906–10.
46. Mahal K, Biersack B, Caysa H. Combretastatin A-4 derived imidazoles show cytotoxic, antivascular, and antimetastatic effects based on cytoskeletal reorganisation. Invest New Drugs 2015;33:541–54.
47. Schwartz EL. Antivascular actions of microtubule-binding drugs. Clin Cancer Res 2009;15:2594–601.
48. Lauffenburger DA, Horwitz AF. Cell migration: a physically integrated molecular process. Cell 1996;84:359–69.
49. Yamaguchi H, Condeelis J. Regulation of the actin cytoskeleton in cancer cell migration and invasion. Biochim Biophys Acta 2007;1773:642–52.
50. Curren RD, Harbell JW. Ocular safety: a silent (*in vitro*) success story. Alt Lab Anim 2002;30:69–74.
51. Deryugina EI, Quigley JP. Chick embryo chorioallantoic membrane model systems to study and visualize human tumor cell metastasis. Histochem Cell Biol 2008;130:1119–30.
52. Ribatti D, De Falco G, Nico B, Ria R, Crivellato E, Vacca A. *In vivo* time-course of the angiogenic response induced by multiple myeloma plasma cells in the chick embryo chorioallantoic membrane. J Anat 2003;203:323–8.

AACR American Association for Cancer Research

Molecular Cancer Therapeutics

Animacroxam, a Novel Dual-Mode Compound Targeting Histone Deacetylases and Cytoskeletal Integrity of Testicular Germ Cell Cancer Cells

Gustav Steinemann, Alexandra Dittmer, Weronika Kuzyniak, et al.

Mol Cancer Ther 2017;16:2364-2374. Published OnlineFirst August 24, 2017.